MAY 1978 PPPL-1422
UC-20f

TRITIUM PERMEATION AND WALL LOADING IN THE TFTR VACUUM VESSEL

BY

JOSEPH L. CECCHI

PLASMA PHYSICS LABORATORY

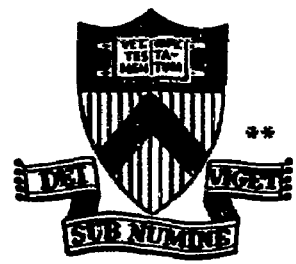

PRINCETON UNIVERSITY
PRINCETON, NEW JERSEY

This work was supported by the U. S. Department of Energy Contract No. EY-76-C-02-3073.

Tritium Permeation and Wall Loading in the TFTR Vacuum Vessel

Joseph L. Cecchi

Plasma Physics Laboratory, Princeton University,

Princeton, New Jersey 08540

ABSTRACT

The problems of tritium permeation through and loading of the TFTR vacuum vessel wall structural components are considered. A general analytical solution to the time dependent diffusion equation which takes into account the boundary conditions arising from the tritium filling gas as well as the source function associated with implanted energetic charge exchange tritium is presented. Expressions are derived for two quantities of interest: (1) the total amount of tritium leaving the outer surface of a particular vessel component as a function of time, and (2) the amount retained as a function of time. These quantities are evaluated for specific TFTR operating scenarios and outgassing modes. The results are that permeation through the vessel is important only for the bellows during discharge cleaning if the wall temperature rises above ~150°C. At 250°C, after 72 hours of discharge cleaning 195 Ci would be lost. The wall loading is most severe in the stainless steel plate sections during normal pulsed operation where 595 Ci would be

retained after 1000 shots if the walls were at 20°C. Maintaining the temperature of the walls above 100°C greatly lessens the problem. The 595 Ci in the wall would be reduced to ~ 10 Ci if the wall were heated to 250°C for about 60 hours.

I. INTRODUCTION

Because hydrogen isotopes are soluable in most metals, the intended use of tritium in the Tokamak Fusion Test Reactor[1] (TFTR) has necessitated careful scrutiny of the mechanisms by which tritium can either be lost from the vacuum vessel by permeation or retained in the vessel walls. The amount of tritium lost by permeation impacts the design of the tritium handling system, since a means for collecting the permeated tritium outside the vessel may be required. Similarly, the amount of tritium retained in the wall and liner components affects the operating scenario, because the total on-site tritium inventory is limited. It is also critical in determining the procedure for disassembly, i.e., how much time must be spent in desorbing the tritium so that the components can be safely handled.

In TFTR there are two important sources of tritium for which permeation and retention in the vacuum vessel components must be considered. The first source is the gaseous molecular tritium which is introduced into the vacuum vessel for tritium operations. In this case the walls would be subjected to a partial pressure of tritium of the order of 10^{-3}T. Some tritium will be adsorbed on the surface and subsequently dissociate and dissolve in the metal. As will be seen, the density of such dissolved tritium depends critically on wall temperature and increases as $(\text{pressure})^{1/2}$. The dissolved tritium will then diffuse at a rate which increases rapidly

with temperature. For thin wall elements such diffusion will transport the tritium to the outside surface where it then reassociates and desorbs. For thicker wall elements the amount transported to the outside surface is negligible, however a certain amount will remain in these elements after a tritium operation is terminated. This retained inventory will continue to diffuse with most of the tritium going to the inside (vacuum) surface and a small fraction moving farther into the metal at rates which increase with temperature.

The second source is the charge exchange neutral tritium flux which is incident upon the vessel walls with a most probable energy of ~ 300 eV. These energetic tritons are implanted directly in the walls to a depth of ~ 600 Å. For this source the adsorption, dissociation, and dissolution steps (which occurred for the gaseous tritium source) are bypassed.

Under certain assumptions, which will be described subsequently, the behavior of the tritium density distribution in a solid is governed by a diffusion equation referred to as Fick's second law.[2] Although the literature contains numerous solutions to this equation,[2-4] no one source includes the analysis required for all types of tritium diffusion problems encountered in TFTR. Therefore, for completeness, we derive in Sec. II a general analytical solution which utilizes boundary conditions to account for the gaseous tritium source, an initial condition to account for cases where tritium is initially found in the material, and an

inhomogeneous term appropriate for the energetic charge exchange source.

In Sec. III formulae for the total retained inventory as a function of time and the total amount of tritium lost from the vessel are derived from the general solution. These quantities are then evaluated for specific vacuum vessel elements in Sec. IV for various modes of operation including discharge cleaning, normal pulsing, and outgassing.

One assumption that will be made in this work is that each of the wall components is free from an oxide layer. In fact, a few hundred angstrom thick oxide coating has been inferred experimentally on PLT by Dylla and Cohen.[5] The diffusion coefficient for tritium in an oxide is quite different than that in a metal, as are the details of dissolution (there is no dissociative step). The problem of such a composite wall involves a nonlinear matching condition, and the time-dependent analytical solution has not yet been found. Although the steady state solution has been obtained,[6,7] we find that at all but the highest temperatures, steady state is not reached in the time of typical operations. A number of authors have experimentally investigated the effect of oxides on permeation.[8-12] Though their conclusions are rather diverse, certain common elements do emerge. An oxide free from cracks or chemical reduction does reduce the rate of permeation over that for a clean metal. The chemical stability of most oxides is not certain; however, and thermal stresses often open cracks which allow some of the diffusing species to bypass

the oxide. The clearest fact is that the effect of an oxide depends critically on its thickness, composition, and integrity, all of which can change, and all of which are unknown a priori. Therefore, although it is recognized that some components may have oxide layers, no attempt has been made to include its effects in the present calculations. Tritium loss rates thus obtained are therefore upper limits, which for the purpose of estimating the amount of tritium lost from the vessel will be desirably conservative.

For estimating the amount retained the oxide would tend to aggrevate the situation by slowing down the back diffusion. However, as we will see, the particular component for which the retention is most severe (and permeation is not a problem) is also one which is subjected to the energetic charge exchange bombardment, and it is possible that much or all of the oxide layer will be sputtered away. Thus, in neglecting the effect of oxides for this case, realistic retention estimates may still be made.

In addition to excluding the effects of oxides, the present calculations also exclude the effects of blistering[13] and/or lattice damage[14] which may occur as a result of the bombardment of a solid by energetic particles. When lattice damage occurs, trapping sites are produced. These sites usually have activation energies greater than that for interstitial diffusion so that the retention problem can be more severe. Fortunately, as is demonstrated in Sec. V, the energy spectrum, flux, and fluence of the charge exchange

particles are such that neither blistering nor lattice damage due to the charge exchange flux should be a problem. The unabsorbed fraction of the 120 keV neutral deuterium beams used to provide auxiliary heating in TFTR can be expected to produce some lattice damage and blistering, however, and Sec. V includes a discussion of how this might affect the tritium problem.

II. GENERAL SOLUTION FOR THE TRANSPORT OF TRITIUM IN NON-REACTIVE METALS

Although the transport of tritium in non-reactive metals includes a number of distinct steps[2,15] (e.g. adsorption, dissociation, dissolution, interstitial diffusion, etc.) depending upon the source of tritium, for the cases encountered in TFTR, interstitial diffusion is the rate determining step. Consequently we may assume that all of the other processes are in their respective equilibria and deal with them in terms of boundary conditions. The concentration of the diffusing species in the metal can be found under these conditions from Fick's second law[2] which is a diffusion equation to which we will add a suitable source term to account for implanted tritium. This can be written for the one dimensional case appropriate to the TFTR vacuum vessel walls as

$$\frac{\partial n(x,t)}{\partial t} + \frac{\partial j(x,t)}{\partial x} = S(x,t) \quad , \tag{1}$$

where $n(x,t)$ is the tritium concentration at the point x at time t, $S(x,t)$ is a tritium source function, and $j(x,t)$ is the diffusional flux given by Fick's first law:[2]

$$j(x,t) = -D\frac{\partial n(x,t)}{\partial x} \quad , \tag{2}$$

with D the diffusion coefficient (diffusivity), assumed to be independent of x and t. The surfaces of the metal are at $x=0$ and $x=d$. In order to obtain unique solutions to Eq. (1) we require a set of initial and boundary conditions. For an initial concentration in the metal $n_o(x)$ we have that

$$n(x,0) = n_o(x) \quad , \tag{3}$$

and we can write the boundary conditions

$$n(0,t) = n_1(t) \quad , \tag{4}$$

$$n(d,t) = n_2(t) \quad , \tag{5}$$

where $n_1(t)$ and $n_2(t)$ are the respective surface concentrations. Under the previously mentioned equilibrium assumptions, these concentrations are given by Sievert's law[2] which relates surface concentration n_s to gas pressure P and solubility S as

$$n_s = SP^k \quad . \tag{6}$$

The exponent k is 1/2 for dissociative diffusion (the case of hydrogen isotopes in metals) and 1 for non-dissociative diffusion.

To solve Eq. (1) subject to the conditions of Eqs. (3) - (5), we first find the Green's function $G(x,t|x_o,t_o)$ which satisfies the equation

$$\frac{\partial G(x,t|x_o,t_o)}{\partial t} - D\frac{\partial^2 G(x,t|x_o,t_o)}{\partial x^2} = \delta(x-x_o)\delta(t-t_o) , \quad (7)$$

subject to the homogeneous boundary condition

$$G(0,t|x_o,t_o) = G(d,t|x_o,t_o) = 0 , \quad (8)$$

and the usual causality requirement

$$G(x,t|x_o,t_o) = 0 \quad t < t_o . \quad (9)$$

The solution to Eq. (1) is then given by [16]

$$\begin{aligned} n(x,t) = &\int_0^d dx_o \int_0^{t^+} dt_o\, G(x,t|x_o,t_o)\, S(x_o,t_o) \\ &+ D\int_0^{t^+} dt_o\, n_1(t_o)\frac{\partial G(x,t|x_o,t_o)}{\partial x_o}\bigg|_{x_o=0} - n_2(t_o)\frac{\partial G(x,t|x_o,t_o)}{\partial x_o}\bigg|_{x_o=d} \\ &+ \int_0^d dx_o\, n_o(x_o)\, G(x,t|x_o,0) , \end{aligned} \quad (10)$$

where the integration limit t^+ is understood to mean $\lim_{\varepsilon\to 0}\int^{t+\varepsilon}$. The first term on the right side of Eq. (10) is the particular solution to Eq. (1) for the source function $S(x,t)$, while the second term gives that part of the solution to the homogeneous equation satisfying the boundary conditions Eqs. (4) and (5), and the third term gives that part satisfying the initial condition Eq. (3).

The Green's function which satisfies Eqs. (7) - (9) is

$$G(x,t|x_o,t_o) = U(t-t_o)\frac{2}{d}\sum_{m=1}^{\infty} \exp[-m^2\alpha\,(t-t_o)]\sin(mkx)\sin(mkx_o), \quad (11)$$

where $\alpha = \pi^2 D/d^2$, $k = \pi/d$, and

$$U(t-t_o) = \begin{cases} 0 & t < t_o \\ 1 & t > t_o \end{cases} . \quad (12)$$

Substituting Eq. (11) into Eq. (10) and assuming that $n_1(t_o)$ and $n_2(t_o)$ are independent of time, we get that

$$n(x,t) = \int_0^d dx_o \int_0^{t^+} dt_o\; G(x,t|x_o,t_o)S(x_o,t_o) +$$

$$\frac{2\alpha^2}{\pi}\sum_{m=1}^{\infty} m(n_2\cos m\pi - n_1)\sin(mkx)\int_0^{t^+} dt_o\, U(t-t_o)\exp[-m^2\alpha\,(t-t_o)]$$

$$+\frac{2}{d}\sum_{m=1}^{\infty}\sin(mkx)\exp(-m^2\alpha\,t)\int_0^d dx_o\, n_o(x_o)\sin(mkx_o) . \quad (13)$$

The integration in the second term of Eq. (13) can be performed by parts:

$$\int_0^{t^+} dt_o\; U(t-t_o)\exp[-m^2\alpha\,(t-t_o)] = \frac{1}{m^2\alpha}[1-\exp(-m^2\alpha\,t)] , \quad (14)$$

Then simplifying the first term in this expression, we can finally write that

$$
\begin{aligned}
n(x,t) = {} & n_p(x,t) \\
& + n_1 + (n_2 - n_1)\frac{x}{d} \\
& + \frac{2}{\pi}\sum_{m=1}^{\infty}\frac{n_2 \cos m\pi - n_1}{m}\sin(mkx)\,\exp(-m^2\alpha\, t) \\
& + \frac{2}{d}\sum_{m=1}^{\infty}\sin(mkx)\,\exp(-m^2\alpha\, t)\int_0^d dx_o\, n_o(x_o)\sin(mkx_o) \quad , \qquad (15)
\end{aligned}
$$

with the particular solution $n_p(x,t)$ given by

$$
n_p(x,t) = \int_0^d dx_o \int_0^{t^+} dt_o\; U(t - t_o)\,\frac{2}{d}\sum_{m=1}^{\infty}\exp[-m^2\alpha(t - t_o)]\,\sin(mkx)\cdot
$$

$$
\cdot\sin(mkx_o)\; S(x_o,t_o) \; . \qquad (16)
$$

For $S(x_o,t_o) = 0$, Eq. (15) for $n(x,t)$ agrees with the solution to the homogeneous equation given by Perkins.[2]

III. GENERAL FORMULAE

In addressing the tritium problem we are primarily interested in two quantities. The first is the total amount of tritium, $N_T(t)$, contained in a particular vacuum vessel component at time t given by

$$N_T(t) = A \int_0^d n(x,t)\,dx \ , \tag{17}$$

where A and d are respectively the area and thickness of the component and $n(x,t)$ is the tritium concentration. The second quantity of interest is the total amount of tritium released through the vessel in time t, $J_T(t)$, given by

$$J_T(t) = A \int_0^t j(d,t')\,dt' \ , \tag{18}$$

where $j(d,t')$ is the flux of tritium at the outside wall ($x = d$) given by Eq. (2):

$$j(d,t') = -D \left.\frac{\partial n(x,t)}{\partial x}\right|_{x=d} \ , \tag{19}$$

with D the diffusivity.

The tritium concentration $n(x,t)$ in Eq. (17) and (18) is given by Eq. (15). This general solution consists of: (a) terms which depend upon the inside ($x = o$) and outside ($x = d$) boundary conditions, n_1 and n_2, respectively; (b) terms which depend upon the source function $s(x_o,t_o)$; and (c) terms which depend upon

the initial condition $n_o(x_o)$. In order to see clearly the effects of each part of the general solution on the expressions for $N_T(t)$ and $J_T(t)$ we will evaluate Eqs. (17) and (18) for each of the three cases individually. Since the equations are linear, the complete solution will just be the sum of the relevant individual solutions.

A. Case I: $n_o(x_o) = S(x_o,t_c) = 0$

This case with n_1 and/or n_2 non-zero applies to cases where the walls are subjected to gaseous tritium at some partial pressure. The resultant surface concentration will be given by Sievert's Law[2] [Eq. (6)], however for conciseness, we will continue to use the symbols n_1 and n_2. The expression for $n(x,t)$ for Case I is, from Eq. (15)

$$n(x,t) = n_1 + (n_2 - n_1)\frac{x}{d} + \frac{2}{\pi}\sum_{m=1}^{\infty}\frac{n_2(-1)^m - n_1}{m}\sin(mkx)\exp(-m^2\alpha t) \quad , \qquad (20)$$

where $k = \pi/d$ and $\alpha = \pi^2 D/d^2$ with d the thickness of the wall and D the diffusivity. From Eq. (17), we get that

$$N_T(t) = N_\infty\left[1 - \frac{8}{\pi^2}\sum_{m=0}^{\infty}\frac{\exp\left[-(2m+1)^2\alpha t\right]}{(2m+1)^2}\right] , \qquad (21)$$

where

$$N_\infty = n_s \frac{Ad}{2} \quad , \tag{22}$$

and $n_s = n_1 + n_2$ is the total surface concentration. Taking the limit of $N_T(t)$ as $t \to \infty$ (steady state) we see that the quantity N_∞ is the total amount of tritium contained in the wall when steady-state is reached. This can also be seen from Eq.(20) where as $t \to \infty$, the tritium distribution becomes linear, going from n_1 at the inside surface (x=0) to n_2 at outside surface (x=d). Thus the average density is $(n_1 + n_2)/2 = n_s/2$ and since the product Ad is the wall volume, the same interpretation follows. In Fig. 1 is plotted the normalized quantity $N_T(t)/N_\infty$ as a function of αt.

Using Eqs. (18)- (20), we get the following expression for the total amount of tritium released from the outside surface of the wall:

$$J_T(t) = J_\infty\{t + \frac{2}{\alpha} \sum_{m=1}^{\infty} \frac{(-1)^m}{m^2} [1 - \exp(-m^2 \alpha t)]\} \quad , \tag{23}$$

where

$$J_\infty = j_\infty A \quad , \tag{24}$$

and the steady state flux j_∞ is given by

$$j_\infty = \frac{n_1 D}{d} \quad . \tag{25}$$

We have assumed $n_2 = 0$ since we will need this quantity only for this case. Using Sievert's law [Eq. (6)] explicitly we get the familiar form[2]

$$j_\infty = \frac{K P^{1/2}}{d} \quad , \tag{26}$$

where the permeability K is defined as $K = SD$. In Fig. 2 we show $J_T(t)/(J_\infty/\alpha)$ as a function of αt.

B. Case II: $n_1 = n_2 = n_o(x) = 0$.

We turn now to the solution for a non-zero source function. From Eq. (15) and (16) we have that

$$n(x,t) = \int_o^d dx_o \int_o^{t^+} dt_o\, U(t-t_o)\, \frac{2}{d} \sum_{m=1}^{\infty} \exp[-m^2\alpha(t-t_o)] \cdot \sin(mkx) \sin(mkx_o)\, S(x_o,t_o) \quad . \tag{27}$$

The appropriate TFTR source function can be written as a product of a spatial part $X(x_o)$ and a temporal part $T(t_o)$. If we now define

$$X_m = \frac{1}{d} \int_o^d dx_o \sin(mkx_o) S_1(x_o) \quad , \tag{28}$$

and

$$T_m = \frac{m^2\alpha}{1-\exp(-m^2\alpha t)} \int_o^{t^+} dt_o\, U(t-t_o) S_2(t_o) \exp[m^2\alpha(t-t_o)], \tag{29}$$

where we have chosen the definitions for later convenience, Eq. (27) may be written as

$$n(x,t) = \frac{2}{\alpha} \sum_{m=1}^{\infty} \frac{S_m}{m^2} \sin mkx\, [1 - \exp(-m^2\alpha t)] \quad , \tag{30}$$

where $S_m = X_m T_m$. Using Eq. (17) we have

$$N_T(t) = N'_\infty \left[1 - \frac{1}{R_1} \sum_{m=0}^{\infty} \frac{S_{2m+1}}{(2m+1)^3} \exp[-(2m+1)^2\alpha t] \right], \tag{31}$$

where

$$N'_\infty = n'_s \frac{Ad}{2} \quad , \tag{32}$$

and

$$n_s' = \frac{8}{\pi}\frac{R_1}{\alpha} \quad , \tag{33}$$

with

$$R_1 = \sum_{m=0}^{\infty} \frac{S_{2m+1}}{(2m+1)^3} \quad . \tag{34}$$

From Eq. (18) we find that

$$J_T(t) = J_\infty' \left[t + \frac{1}{\alpha R_2} \sum_{m=1}^{\infty} \frac{(-1)^m S_m}{m^3} (1 - \exp(-m^2 \alpha t)\right] \quad , \tag{35}$$

where

$$J_\infty' = j_\infty' A \quad , \tag{36}$$

and

$$j_\infty' = \frac{2d}{\pi} R_2 \quad , \tag{37}$$

with

$$R_2 = \sum_{m=1}^{\infty} \frac{(-1)^{m+1} S_m}{m} \quad . \tag{38}$$

Eqs. (31) and (35) are written in a way to suggest a formal similarity to the analogous formulae [Eqs. (21) and (23)] for the boundary value case. For $t \to \infty$. the quantity n_s' is the effective surface concentration associated with the source $S(x_o, t_o)$. The total accumulation in the metal at $t \to \infty$ due to the energetic implantation described by $S(x_o, t_o)$ is equivalent to that for a surface concentration given by n_s' in Eq. (33). One important difference, however, is that n_s' is inversely proportional to D .[17] Since D increases with temperature, the maximum total accumulation for an implanted distribution decreases with temperature, whereas the maximum total accumulation

for the boundary value case is proportional to n_s which is given by Sievert's law and which increases with temperature. j'_∞ of Eq. (37) is the equivalent steady state flux. Unlike the steady state flux for the boundary value case which is proportional to the product of solubility and diffusivity, j'_∞ is independent of diffusivity and therefore of temperature.[17] For finite t, there is no obvious formal similarity between the implantation case and the boundary condition case because the terms in the sums are weighted differently.

The spatial part of the source function $X(x_o)$ has been derived by Cohen and Marmar[18] who calculated the energetic deposition profile of the charge exchange tritium atoms for the high power pulse case. The calculation assumes an ion temperature of 3 keV and peak plasma density of $10^{14}cm^{-3}$. The calculated distribution is shown in Fig. 3. In Fig. 4 is shown a triangular distribution which will be used to approximate the calculated distribution in Fig. 3. In the triangular distribution the peak (S_p) occurs at $x = b$ and $x = c$ is the end of range. Values of S_p, b and c for the high power pulse case are listed in the insert for this figure. The deposition profile for discharge cleaning depends upon the type of cleaning. We will consider only agressive discharge cleaning, since it represents a worst case for the tritium problem. We will utilize a triangular distribution with the parameters listed in Fig. 4. The assumptions involved in calculating these parameters are that the incident flux is $3 \times 10^{15}cm^{-2}sec^{-1}$, the backscatter probability

is .9, and the mean energy of the neutrals (or ions) is ~ 30 eV.

The time factor $T(t_o)$ is shown graphically in Fig. 5. For convenience we take $T(t_o)$ to be dimensionless and include the rate in S_p. With suitable choices for $\Delta\tau$ and τ it can be used for both the normal pulsed case and discharge cleaning. If we consider a sequence of N pulses and evaluate Eq. (29) for times longer than the duration of the sequence $[t > (N-1)\tau + \Delta\tau]$ we have that

$$T_m = \frac{m^2\alpha}{1-\exp(-m^2\alpha t)} \sum_{n=0}^{N-1} \int_{n\tau}^{n\tau+\Delta\tau} dt_o\, U(t-t_o)\, \exp\,(-m^2\alpha(t-t_o)$$

$$= \frac{\exp(-m^2\alpha t)}{1-\exp(-m^2\alpha t)} \left[\exp(m^2\alpha\Delta\tau)-1\right] \sum_{n-0}^{N-1} \exp\,(m^2\alpha n\tau) \quad . \tag{39}$$

Performing the summation in Eq. (39) we get that

$$T_m = \frac{\exp(-m^2\alpha t)}{1-\exp(-m^2\alpha t)} \left[\exp(m^2\alpha\Delta\tau)-1\right] \frac{\exp(m^2\alpha N\tau)-1}{\exp(m^2\alpha\tau)-1} \quad . \tag{40}$$

The instantaneous values of $N_T(t)$ and $J_T(t)$ will show variations on short time scales during each pulse. What we are actually interested in is some average of these quantities. We can acomplish this and realize a simplification in the preceeding equation by letting $t = N\tau$ in Eq. (40). Strictly speaking, t becomes a discrete variable, however we will treat it as continuous since, for large N the increment is small. The resulting expressions will then be smoothed functions. The general solution can be easily obtained by using $n(x, N\tau)$ in the initial value case described in Section III C in order to obtain results for

arbitrary values of t .

Letting $t = N\tau$, Eq. (40) becomes

$$T_m = \frac{\exp(m^2\alpha\Delta\tau)-1}{\exp(m^2\alpha\tau)-1} , \qquad (41)$$

T_m is shown normalized by $t/\Delta\tau$ as a function of $m^2\alpha\tau$ in Fig. 6. For $\Delta\tau = \tau$, $T_m = 1$ for all values of $m^2\alpha\tau$. This is the continuous-flux case. For the TFTR situation, $\Delta\tau/\tau \lesssim .1$. In this case T_m cuts off sharply for $m^2\alpha\tau \gtrsim 10$. If the sums R_1 and R_2 [Eqs. (34) and (38)] are cut off at $m = (10/\alpha\tau)^{1/2}$ the resulting fractional errors are less than 10^{-3} using standard analysis.[19] For $m < (1/\alpha\tau)^{1/2}$, we see that T_m is approximately equal to the duty factor $\Delta\tau/\tau$. For all of the m components such that $m < (1/\alpha\tau)^{1/2}$, no appreciable changes take place between successive machine pulses so that it is equivalent to the steady state case with a time-averaged flux.

The behavior of X_m is somewhat more complicated. Performing the integration in Eq. (28) we find that

$$X_m = \frac{S_p}{\pi^2 m^2} \frac{d}{c-b} \left[\frac{c}{b} \sin\left(\frac{m\pi b}{d}\right) - \sin\left(\frac{m\pi c}{d}\right)\right], \qquad (42)$$

where b, c, d are the distances to the peak of the distribution, the end of range, and the outside surface respectively as shown in Fig. 4. Using the ratio of b to c of 1/5, X_m is graphed in Fig. 7, normalized by the factor $d/(S_p c)$.

There is an initial linear behavior up to $m(b/d) \sim .1$ given by

$$X_m \simeq S_p \frac{m\pi}{6} \frac{c(c+b)}{d^2} \quad . \tag{43}$$

For larger values of m the function is oscillatory, bounded by an envelope which scales as $\sim (mb/d)^{-2}$.

In situations where

$$\left(\frac{10}{\alpha\tau}\right)^{1/2} < \frac{d}{10b} \quad , \tag{44}$$

the cut-off due to T_m occurs in the linear region of X_m and the sum can be simplified considerably by using Eq.(43) for X_m. Another useful approximation can be used when the sums involve sufficient additional inverse powers of m to cause the series to converge in the linear region of X_m ($m < d/10\,b$) and in the constant region of T_m ($m \leq (1/\alpha\tau)^{1/2}$). In such cases the sum reduces to a sum over inverse powers of m. A detailed analysis of the remainder is necessary to determine when such an approximation may be made.

C. Case III: $n_1 = n_2 = S(x_o, t_o) = 0$

After a given distribution of tritium is established within some vacuum vessel element (due to either tritium gas in contact with the surface or energetic implantation) it is of interest to determine the subsequent evolution of the tritium after the source is terminated. This outgassing mode requires the initial value formalism which is given by Eq. (15) as

$$n(x,t) = \frac{2}{d} \sum_{m=1}^{\infty} \sin(mkx) \exp(-m^2 \alpha t) \int_0^d dx_o \, n_o(x_o) \sin(mkx_o) \quad , \qquad (45)$$

where $n_o(x_o)$ is the distribution at $t = 0$. We will be interested in two forms of $n_o(x_o)$. For the boundary value case, we will consider the subsequent evolution only after the distribution has reached steady-state so that from Eq. (20) we get that

$$n_o(x_o) = n_1 \left(1 - \frac{x_o}{d}\right). \qquad (46)$$

In this case Eq. (45) becomes

$$n(x,t) = \frac{2}{\pi} \sum_{m=1}^{\infty} \frac{n_1}{m} \sin(mkx) \exp(-m^2 \alpha t) \quad . \qquad (47)$$

In a straightforward manner we get from Eq. (17) that

$$N_T(t) = N_\infty \frac{8}{\pi^2} \sum_{m=0}^{\infty} \frac{1}{(2m+1)^2} \exp[-(2m+1)^2 \alpha t] \quad , \qquad (48)$$

where $t = 0$ corresponds to the time when the tritium source was terminated. Note that $N_T(0) = N_\infty$ so that it matches Eq. (21) (the latter at $t \to \infty$). This function is plotted in Fig. 8.

From Eq. (18) we get that

$$J_T(t) = J_\infty \frac{2}{\alpha} \sum_{m=1}^{\infty} \frac{(-1)^{m+1}}{m^2} [1 - \exp(-m^2 \alpha t)] \quad . \qquad (49)$$

Since

$$\sum_{m=1}^{\infty} \frac{(-1)^{m+1}}{m^2} = \frac{\pi^2}{12} , \tag{50}$$

we find that in the limit $t \to \infty$,

$$J_T(t \to \infty) = \frac{N_\infty}{3} . \tag{51}$$

Thus, if we begin with a steady state distribution, it will evolve such that 1/3 of the total accumulation will leave the outer surface and [since from Eq. (42) $N_T(\infty) = 0$] 2/3 will return to the vacuum.

For the source function case, if the source is on for time t_s and α_s is the rate appropriate to the wall temperature during that time, then from Eq. (30) we have

$$n(x,t) = \frac{2}{\alpha_s} \sum_{m=1}^{\infty} \frac{S_m [1 - \exp(-m^2 \alpha_s t_s)}{m^2} \sin mkx \exp(-m^2 \alpha t) , \tag{52}$$

where we have allowed for different wall temperatures during and after the source being on by using the two rates α_s and α .
Note that $t = 0$ corresponds to the time t_s .
From Eqs. (17) and (18) we find that

$$N_T(t) = \frac{4}{\pi} \frac{Ad}{\alpha_s} \sum_{m=0}^{\infty} \frac{S_{2m+1} [1 - \exp[-(2m+1)^2 \alpha_s t_s]]}{(2m+1)^3} \exp[-(2m+1)^2 (\alpha t)], \tag{53}$$

and

$$J_T(t) = \frac{2}{\pi} \frac{Ad}{\alpha_s} \sum_{m=1}^{\infty} \frac{(-1)^{m+1} S_m [1 - \exp(-m^2 \alpha_s t_s)]}{m^3} [1 - \exp(-m^2 \alpha t)] . \tag{54}$$

IV. SPECIFIC RESULTS

The TFTR vacuum vessel is constructed in ten segments with each segment including thin (~ 1.1 mm) corrugated bellows sections (for high electrical resistivity) and thick (~ 1.3 cm) plate sections. A complete description of the vessel can be found in Ref. 1. The insides of the bellows sections are covered by protective plates and thus shielded from bombardment by the energetic charge exchange particles and the unabsorbed fraction of the 120 keV neutral beams used for heating in TFTR. Protective plates also shield portions of the solid plate sections from the unabsorbed portion of the 120 keV beams. The problem of tritium permeation and retention will be considered for each of these three vacuum vessel components. Table I lists the relevant physical parameters for them. At present neither the material nor size of the protective plates has been specified. For the present calculation we will assume that they will be fabricated out of molybdenum. The other parameters listed for the protective plates in Table I represent the current best estimates.

In Table II are listed the values for the permeability K , diffusivity D, and solubility S which are required to evaluate the formulae in Sec. III for the specific TFTR vacuum vessel components. Each of the coefficients is presented in an Arrenhius form: A exp (-B/RT) with temperature T (°K), pre-exponential factor A (K_o, D_o, and S_o for K, S, and D respectively), and activation energy B(Q_K, Q_D, and Q_S for K, S, and D respectively). For the plate sections the 304 L SS values[22] will be used, while the Mo values[2, 23, 24]

will be used for the protective plates. In each of these cases, the solubility pre-exponential factor and activation energy was derived from the experimentally determined K and D . For the bellows the experimentally determined[20] K for Inconel 625 will be used. The other coefficients for Inconel 625 have not yet been measured, however, so that the solubility of single crystal nickel[21] will be used with the permeability of Inconel 625[20] to determine D for the bellows. The value of D which results from the calculation is within a factor of 2 of those measured for Ni - Fe alloys with 50% (by weight) Ni,[25] which is the same percentage of Ni that is in Inconel 625. This will not affect the steady state permeation rate since it depends only upon K, although the time to reach steady state does depend upon D . All of the data in Table II are for hydrogen permeation. No attempt has been made to correct for the tritium mass difference.

We will be interested in two basic scenarios. The first is discharge cleaning for which we will assume that the vessel is filled with tritium at a pressure of 10^{-3}T for the duration of the run. The length of a typical run will be assumed to be 72 hours. The characteristics of the charge exchange flux are given in Figs. 4 and 5. The second situation of interest is the normal pulsed operation. Here the torus will be filled by a pulsed gas valve prior to each discharge so that the time averaged background tritium pressure will be small, and this source can be ignored. The major source of tritium will be the charge exchange flux, the parameters of which are shown in Figs. 4 and 5. The

present plans allow for 1000 high power tritium discharges per year, and it is anticipated that these will occur in ten 100 shot runs.

A. Bellows

Since the bellows are shielded from the energetic tritium charge exchange flux, we need to consider only the background tritium at a partial pressure $\sim 10^{-3}$ T which is present during discharge cleaning. Using the values of D and S in Table II and Eq. (21), the total trapped inventory as a function of time is plotted in Fig. 9 for T = 20°C, 150°C, and 250°C with a partial pressure of 10^{-3}T. It is obvious from Fig. 9 that the wall loading of the bellows is an insignificant problem at 20°C where the loading after 1000 hrs. is only ~ 1 Ci At the two elevated temperatures (150° C and 150°C) the respective steady state accumulations are 22 Ci and 43 Ci attained in times between 10 and 100 hours. While considerably larger than at room temperature, these accumulations are still relatively small. In the highest temperature case, after the tritium pressure goes to zero, if the walls remain at 250°C for ~ 7 hours, the total accumulation will fall to below 1 Ci as can be determined from Fig. 8. In this case ~ 14 Ci will permeate to the outer surface and~28 Ci will return to the vacuum. A similar reduction to < 1 Ci will occur for the 150° C case if the walls remain at that temperature for ~ 50 hours following discharge cleaning.

To determine the quantity which permeates the bellows during discharge cleaning, we use Eq. (23) for the same cases as considered previously. The results are shown in Fig. 10. Steady state permeation (i.e. $J_T \propto t$) is reached in 250 hrs. at 150°C and 25 hrs. at 250°C. After 72 hrs. at 250°C the total quantity leaving the vessel is 195. Ci .

B. Plate Sections

In the case of the stainless steel plate sections we will separately consider discharge cleaning where a background pressure of tritium plus a charge exchange flux are both present and also normal pulsed operation, where the background tritium is an insignificant source but where the energetic charge exchange is important. In both cases, however, the plate sections are sufficiently thick so that the total flux through the wall is insignificant. In the case of discharge cleaning at 250°C with a tritium pressure of 10^{-3}T, after 5000 hours, the total quantity of tritium which would permeate the plate sections is ~ .05 Ci. To estimate an upper limit on the outflux due to the energetic charge exchange, we use the result of Cohen and Marmar[18] which is that when steady state is reached, the ratio of the flux through the outer wall to that through the inner wall is equal to the distance of the tritium from the inner wall divided by the distance to the outer wall. If we assume all of the tritium penetrated to the 600 Å end of range, then the fraction of the incoming flux which diffuses to the outer wall (in steady state) is ~ $5 \times 10^{-6}/1.27 = 4.7 \times 10^{-6}$. The total flux during the pulse through the plate section area is ~ $10^{15}\text{cm}^{-2}\text{sec}^{-1} \times 9.5 \times 10^{5}\text{cm}^{2} \times 1\ \text{sec} \simeq 10^{21}$ particles pulse^{-1}. Multiplying this by the outflux fraction and converting to Curies we get ~ 10^{-3} Ci pulse^{-1}, an insignificant amount, especially considering that even at 250°C steady state would not be reached for ~ 100 days.

For discharge cleaning with a tritium partial pressure of 10^{-3}T, the total wall loading of the plate sections given by Eq. (21) is plotted in Fig. 11. Because of the thickness of the plate sections; steady state is not reached during typical discharge cleaning runs.

We must also consider the wall loading from the charge exchange flux during discharge cleaning. To do this we resort to Eq. (31). We note, however, that an integral quantity like $N_T(t)$ has three inverse powers of the summation index and will, therefore, converge faster than the corresponding sum for the distribution function. The linear approximation in Eq. (43) holds up to m ~ d/10b which, for the discharge cleaning is ~ 10^6. For all of the temperatures we will consider, the linear region of X_m ($m \lesssim 10^6$) lies within the constant region of T_m where $m \lesssim (1/\alpha\tau)^{1/2}$ with τ = 3 sec. Hence, if the sums in Eqs. (31) and (34) converge rapidly enough so that we can truncate the series at m = d/10b then the summation is considerably simplified. The linear approximation for X_m and constant approximation for T_m yield sums involving $1/m^2$ which are similar to those encountered in the boundary condition case where the tritium source was a gas at some pressure [Eq. (21)]. Detailed error analyses[19] of the truncated series in Eqs. (31) and (34) show that the error decreases with time. In particular, for time t such that t ~ 6τ, the error introduced by truncating the series is 10%. For t ~ 600 τ the error is 1%. One remaining simplification is to use the infinite sums in Eq. (21). This introduces an error equal to or less than that introduced by the truncation, i.e., a total error of 20% for t ~ 6 τ and 2% for t ~ 600 τ. These approximate results are plotted in Fig. 12 from t = 6 τ. At the

lowest temperature (20°C) t e wall loading from the charge exchange flux greatly exceeds that from the background filling gas. It also dominates the loading of the bellows. At 150°C, however, the diffusivity is high enough to reduce the amount of charge exchange tritium retained while the greater solubility increases the loading from the filling gas, so that the background gas source dominates over the charge exchange source at this temperature. At the highest temperature (250°C) the charge exchange loading is negligible while after 72 hours the filling gas loading of the plate section is almost double that of the bellows.

For normal pulsed operation we will consider in detail various outgassing modes in addition to calculating the quantity retained. For the latter we will use Eq. (31) with approximations analogous to those made for discharge cleaning. For outgassing calculations we will use Eq. (53). A number of typical scenarios are depicted in Fig. 13. It is assumed that the device is pulsed for 1 second every 300 seconds with a tritium charge exchange flux resulting in the deposition profile approximated in Fig. 4. All quantities relating to the implant operations are time averaged in the sense that their values just prior to each discharge is plotted and connected smoothly to those values for the previous and succeeding pulses. [See discussion following Eq. (40)]. The total retained quantities for 20°C and 250°C walls are plotted along with outgassing modes at 20°C and 250°C for 100, 1000, and 10,000 discharges.

As was observed for discharge cleaning, the total retained quantity is greater at 20°C than at 250°C (due to

the lower diffusivity at 20°C) and in each case increases as $t^{1/2}$ in the region of interest.

As an example of a typical outgas mode, consider the 250°C case after 100 discharges at 20°C. Initially upon increasing the temperature from 20°C to 250°C there is a very rapid (almost exponential) decrease in $N_T(t)$. This occurs because the exponential factor in the sum in Eq. (31) $\{\exp [-(2m + 1)^2 \alpha t]\}$ becomes "operative" for a large number of terms since $\alpha(T = 250°C) >> \alpha(T = 20°C)$. Once these higher m components are attenuated, the outgas mode enters into a second phase (at ~ 30 hrs. for the case being considered) where $N_T(t)$ is proportional to $t^{-1/2}$. This slow fall-off continues until $\alpha t \sim 1$ ($t \sim 2000$ hrs.) when all the component ($m \geq 0$) are strongly attenuated by the $\exp [-(2m +1)\alpha t]$ factor. At this point $N_T(t)$ decreases exponentially to very small values. For the 250°C outgassing after 1000 or 10,000 discharges at 20°C, the middle $t^{-1/2}$ region is barely existent or non-existent. For all the 20°C outgassing modes after 20°C implants, there is no initial rapid attenuation because α is not changed discontinuously. Also the final exponential fall occurs well after 10^5 hours.

If the outgassing temperature is greater than or equal to the implant temperature, then the value of $N_T(t)$ during and after the $t^{-1/2}$ region is independent of the initial wall temperature. This can be seen clearly in the 250°C outgas mode after 100 discharges by comparing the results for the 20°C and 250°C implants.

After 1000 consecutive discharges with 20°C walls, the total retained quantity would be 595 Ci. After ~ 63 hours at 250°C this would be reduced to 10 Ci and after ~ 450 hours it would be reduced to 1 Ci. If the walls had been at 250°C, the total amount after 1000 discharges would be ~ 6 Ci. Of course it is not likely that the device would be operated for 1000 consecutive discharges with τ = 300 sec. The results, assuming that the 1000 discharges are spread over one year, are plotted in Fig. 14. Here $\tau = 3 \times 10^4$ sec. The factor of 100 decrease in the duty factor results in a factor of 10 decrease in N_T, compared to the τ = 300 sec case for the same number of discharges. This follows from the $N_T(t)$ proportional to $t^{1/2}$ behavior. The subsequent 250°C outgas appears to be more rapid, however this is due to the fact that the outgas modes are plotted on the same logarithmic time scale as the implantations.

One other case of interest would be ten - 100 discharge runs with the walls at 20°C, τ = 300 sec and one month between the runs. For 100 discharges at 20°C we have from Fig. 13 an initial retained inventory of ~ 200 Ci. After one month this becomes ~ 14 Ci. After n months at 20°C the retained quantity would be ~ 14 $n^{-1/2}$ Ci. Since 14 Ci is small compared to the 200 Ci build up over a 100 discharge run, the total retained after the ten runs would be approximately given by the sum: $N_T \sim 14 \sum_{n=1}^{10} n^{-1/2}$. The result is ~ 70 Ci.

This is not appreciably different from the 59.5 Ci which would be retained after 1000 shots with $\tau = 3 \times 10^4$ sec (Fig. 14).

C. Protective Plates

The Mo protective plates have ~ 10% the area of the stainless steel plate sections, a greater diffusivity, and a much smaller solubility. As a consequency, the equilibrium loading at 250°C from a 10^{-3}T pressure of tritium is less than 10 mCi. Also, because of the increased diffusivity, the loading from the high power pulsing after 1000 shots at 20°C is ~ 3 Ci. Hence, the amount of tritium contained in the protective plate sections is negligible. If tungsten were used instead of Mo, the total amount would be even less in all cases.[26]

V. SUMMARY AND DISCUSSION

The results of Section IV are summarized in Table III for the cases of a 72 hour discharge cleaning run with a tritium pressure of 10^{-3}T and normal pulsed sequences of 1000 discharges with 300 seconds and 3×10^4 seconds between discharges. Tritium permeation through the bellows is significant during discharge cleaning if the walls reach temperatures above 150°C. In particular, after 72 hours of discharge cleaning with the bellows at 250°C, the total quantity lost would be 195 Ci. If a non-aggressive type discharge cleaning is employed such that the wall temperature stays close to 20°C, however, less than 1 μ Ci would be lost.

Permeation through the bellows during normal pulsed operation is not significant because of the low duty cycle of the filling gas. Also, permeation through the plate sections is not a problem in any mode of operation because of its thickness and the relatively small permeability of stainless steel.

The wall loading problem again depends critically upon temperature. The bellows, during discharge cleaning, will reach saturation for temperatures above 150°C. For 250°C the total trapped inventory would be 43 Ci while at 150°C it is 22 Ci. At 20°C, after 72 hours, only 250 m Ci would be trapped. At the elevated temperature where the internal tritium distribution reaches steady-state a subsequent outgassing would return 2/3 of the trapped inventory to the vacuum and 1/3 would leave the outer bellows surface. The time to reduce the inventory to 1 Ci at 250°C is approximately 25 hours.

The loading of the stainless steel plate sections during discharge cleaning arises from two sources. The first is the filling gas and, as in the bellows case, this increases with wall temperature. Unlike the thin bellows, however, the plate sections do not reach equilibrium in the 72 hours of a discharge cleaning run. The second tritium source is the implantation of charge exchange neutrals. For this source the greatest loading occurs at 20°C because the diffusivity is the lowest and the tritium cannot diffuse away from the implant position very rapidly. Here, also, equilibrium is not reached. After 72 hours the total loading of the plate sections is high at both 20°C and 250°C being 63 Ci and 71 Ci respectively. At 150°C the total is 16 Ci .

During normal pulsed operation, the salient problem is the wall loading of the plate sections from the energetic charge exchange flux. If one considers a 1000 pulse run with 300 seconds between pulses, then if the walls were 20°C, 595 Ci would be retained. If the wall temperature after the run were raised to 250°C, the total accumulation would decrease to ~ 10 Ci in 63 hours with virtually all of the tritium returning to the vacuum vessel. If the 1000 shots were spread over one year ($\tau = 3 \times 10^4$ sec) the retained quantities are reduced by a factor of 10 over the values for $\tau = 300$ sec.

It should be reiterated that all of these results have been derived assuming no oxide layer on the metal surfaces. An oxide layer would be expected to slow the rate of permeation and also increase the wall loading. As discussed in Section I,

however, it is likely that sputtering will eliminate the oxide layer from the plate sections. In the recent experiments of Wilson and Baskes,[27] type 316 stainless steel was bombarded with deuterium at various energies, including 333 eV D^+ at a flux of $6.2 \times 10^{14} cm^{-2} sec^{-1}$ and fluences up to $3 \times 10^{18} cm^{-2}$ (equivalent to ~ 1000 TFTR pulses). They found that for samples with clean surfaces, the observed reemission agreed with the predictions of a simple diffusion calculation similar to that presented here. For "as is" surfaces they did observe some hold-up of the implanted deuterium.

The occurence of blistering due to the tritium charge-exchange bombardment of the plate sections and protective plates could cause deviations from the present predictions for tritium retention. Since blistering causes large releases of implanted gas, the deviations would tend to be salutary with respect to the tritium retention problem though not necessarily so from the point of view of plasma impurity control and tritium recycling. In any case it is appropriate to examine the possibility of blister formation. The onset of blistering seems to be related to the density of implanted particles locally exceeding some solubility limit.[13] Blister formation, therefore, depends upon the flux, fluence, and energy distribution of the implanted source, as well as parameters such as temperature and diffusivity of the material. It has been observed that for given implanted source characteristics, as the temperature of the material is increased, the resulting increased diffusivity reduces blister occurence. The TFTR

tritium charge exchange flux is 3 x $10^{15} cm^{-2} sec^{-1}$ with a broad energy distribution peaked at ~ 300 eV. Unfortunately, there are no data for blister formation due to hydrogen isotope implantation of Mo and SS at such low energies. Verbeek and Eckstein[30] did observe blister formation in Mo and SS due to a 15 keV D^+ beam with the targets at room temperature. The D^+ fluxes were approximately equal to those of the TFTR charge-exchange tritons. The onset for blistering in both cases occurred near fluences of ~ $10^{18} cm^{-2}$ which would correspond to ~ 300 TFTR discharges. For a number of reasons, however, the blister threshold in TFTR will probably be greater than that observed by Verbeek and Eckstein.[30] One reason is that the much broader energy distribution of the charge exchange flux as compared with the mono-energetic 15 keV beam means that the maximum implant density in the TFTR case is much less. Furthermore, the shallower implantation in the TFTR wall means that more implanted particles will escape from the surface, a feature which also reduces the maximum density in the wall.

In addition to blistering we must also consider the possibility that lattice damage resulting from the tritium charge exchange bombardment of the plate sections and protective plates will cause trapping sites with activation energies above those for interstitial diffusion,[14] resulting in increased tritium retention. The data of Wilson and Baskes[27] for clean 316 SS samples would tend to indicate that such trapping is not important. In addition to the

333 eV D^+ bombardment they also studied 1 keV D^+ bombardment observing for clean surfaces similar agreement between theory and experiment, so that even for the higher energy TFTR charge exchange flux, lattice damage should not affect the present results.

Besides being subjected to the tritium charge-exchange flux, the protective plates will also be bombarded by the unabsorbed fraction of the neutral deuterium heating beams. These energetic beam fluxes will cause lattice damage and thus trapping sites. To estimate an upper limit on the number of trapping sites produced we will assume 10% of the 120 keV beam component will be unabsorbed (with suitably scaled fractions of the 60 keV and 40 keV components). The total number of deuterium atoms striking the protective plates per pulse will be: 4.3×10^{18} at 120 keV, 2.1×10^{18} at 60 keV, and 1.2×10^{18} at 40 keV. Extrapolating the results of McCracken and Erents[14] for the damage rate from deuterium bombardment of Mo we get ~ 1.8 defects ion^{-1} at 120 keV, 0.9 defects ion^{-1} at 60 keV, and 0.6 defects ion^{-1} at 40 keV. Although the damage will have a maximum near the end of ranges of the three deuterium energy components, we will assume (as a worst case) that it is spread uniformly over the ranges. Then we can estimate the total number of defects produced in the first 600 Å where the tritium charge exchange neutrals will be implanted by multiplying the defects ion^{-1} by 600 Å divided by the deuterium range[31] for each of the three components.

If we then assume that one half of the traps produced are occupied by the deuterium itself and the remaining one half trap the implanted tritium, we find that .15 Ci/pulse would be retained in the protective plates. Assuming that the rate of defect production remains linear, 150 Ci would be retained after 1000 pulses. This figure is included in Table III, although it is probably an overestimate for the previously stated reasons that 10% unabsorbed beam is rather high and the number of defects produced in the first 600 Å will likely be less than assumed. Of course the higher activation energy of these damage produced traps[14] will make thermal desorption more difficult, so that to remove this retained tritium might require either deuterium discharge cleaning or high power pulses in deuterium.

Blister formation due to 120 keV, 60 keV, and 40 keV D^+ bombardment of Mo has been investigated by Kaminsky et al.[29] They find extensive blistering at room temperature, but an absence at 300°C. The dominant result of such blistering would be increase reemission of the deuterium, although an increase in the reemission of tritium trapped in damage sites may occur also.

ACKNOWLEDGEMENTS

I would like to acknowledge a number of stimulating and profitable discussions with S. A. Cohen, D. K. Owens, M. Kaminsky, G. Lewin, and H. F. Dylla.

This work was supported by U.S.D.O.E., Contract EY-76-C-02-3073.

REFERENCES

[1]Tokamak Fusion Test Reactor, Report PPPL-1312, Plasma Physics Laboratory, Princeton University, Princeton, N. J. (1976) unpublished.

[2]W. G. Perkins, J. Vac. Sci. Technol. 10 (1973) 543.

[3]W. D. Wilson, C. J. Bisson, and D. E. Amos, J. Nucl. Mater. 53 (1974) 154.

[4]K. Erents and G. M. McCracken, Brit. J. Appl. Phys. (J. Phys. D.) 2 (1969) 1397.

[5]H. F. Dylla and S. A. Cohen, J. Nucl. Mater. 63 (1976) 487.

[6]R. Aronson, L. S. Castleman, and K. Chung, Report P(TOK)-ACC-2, Polytechnic Institute of New York, Brooklyn, 1977, (unpublished).

[7]W. G. Perkins, in Effect of Hydrogen on the Behavior of Materials, Thompson, A. W. ed., (Metallurgical Society of AIME, New York, 1976) 355.

[8]R. A Strehlow and H. C. Savage, Nuclear Tech. 22 (1974) 127.

[9]W. A. Swansiger, in International Conference on Radiation Effects and Tritium Technology for Fusion Reactors, Gatlinburg, 1975, (NTIS, Springfield, Va., 1976) IV-401.

[10]J. D. Fowler Jr., R. A. Causey, D. Chambra, T. S. Ellerman, and K. Verghese, J. Vac. Sci. Technol. 13, (1976) 402.

[11]J. H. Austin and T. S. Ellerman, J. of Nucl. Mater. 43 (1972) 119.

[12]W. A. Swansiger, R. G. Musket, L. J. Weirick, and W. Bauer, Report SLL-74-0208, Sandia Laboratories, Livermore, CA. 1974 (unpublished).

[13]S. K. Das and M. Kaminsky, Adv. in Chem. 158 (1976) 112.

[14]G. M. McCracken and S. K. Erents, in International Conference on Applications of Ion Beams to Metals, Albuquerque, N. M., 1973, S. T. Picraux, E. P. Eer Nisse, and F. L. Vook eds., (Plenum Press, New York, 1974) 585.

[15]R. E. Stickney, in Chemistry of Fusion Technology, D. M. Gruen ed. (Plenum, New York, 1972) 241.

[16]P. M. Morse and H. Feshbach, Methods of Theoretical Physics, (McGraw-Hill, New York, 1953) 806.

[17]It will be seen subsequently that n_s' and j_∞' may depend upon D weakly through S_{2m}. This does not affect the dominant behavior described here, however.

[18]S. A. Cohen and E. S. Marmar, Report TM-286, Plasma Physics Lab., Princeton University, Princeton, N. J. (1975) unpublished.

[19]G. Dahlquist and A. Bjorck, Numerical Methods (Prentice-Hall, Inc. Englewood Cliffs, N. J., 1974) 60.

[20]E. H. Van Deventer, to be published. For a discussion of the experimental method see E. H. Van Deventer, J. of Nucl. Mater. (1977) 325.

[21]W. Eichenauer, W. Läser, and H. Witte, Z. Mettalkd, 56 (1965) 287.

[22]M. R. Louthan, Jr., R. G. Derrick, Corros. Sci. 15 (1975) 565.

[23]R. Frauenfelder, J. Chem. Phys. 48 (1967) 3955.

[24]W. A. Oates and R. B. McLellan, Sci. Metall. 6 (1972) 349.

[25]W. Beck, J. O'M. Bockris, M. A. Genshaw, and P. K. Subramanyan, Metal. Trans. 2 (1971) 883.

[26]R. Frauenfelder, J. Vac. Sci. Technol. 6 (1969) 388.

[27]K. L. Wilson and M. I. Basken, J. Nucl. Mater. (to be published).

[28]K. L. Wilson, G. J. Thomas, and W. Bauer, Nucl. Technol. 29 (1976) 322.

[29]M. Kaminsky, S. K. Das, and P. Duza, Report ANL/FPP TM/105, Argonne National Laboratory, Argonne, Illinois (1978) unpublished.

[30]H. Verbeek and W. Eckstein, in International Conference on Applications of Ion Beams to Metals, Albuquerque, N. M., 1973, S. T. Picraux, E. P. Eer Nisse, and F. L. Vook eds., (Plenum, New York, 1972) 597.

[31]J. Linhard and M. Scharff, Phys. Rev. 124 (1961) 128.

TABLE I.

VACUUM VESSEL COMPONENT SPECIFICATIONS

VACUUM VESSEL COMPONENT	MATERIAL	AREA (cm^2) (A)	THICKNESS (cm) (d)
BELLOWS	INCONEL 625	1.5×10^6	0.114
PLATE SECTIONS	SS 304LN	9.5×10^5	1.27
PROTECTIVE PLATES	Mo	1.3×10^5	1.27

TABLE II.

PERMEABILITIES, DIFFUSIVITIES, AND SOLUBILITIES FOR VACUUM VESSEL MATERIALS

MATERIAL	$10^3 K_o$ (a)	Q_K (b)	$10^3 D_o$ (c)	Q_D (b)	S_o (d)	Q_S (b)
Inconel 625 (e)	19.7	14.4	7.6	11.5	2.6	2.9
304L SS (f)	6	14.3	4.7	12.9	1.3	1.4
Mo (g)	24	21.5	4.8	9.0	5.0	12.5

(a) UNITS cm^3(STP) sec^{-1} cm^{-1} $atm^{-1/2}$

(For tritium, to convert to Ci $sec^{-1} cm^{-1} T^{-1/2}$ multiply by 9.36×10^{-2})

(b) UNITS K Cal mol^{-1}

(to convert to eV $atom^{-1}$ multiply by 4.34×10^{-2})

(c) UNITS $cm^2 sec^{-1}$

(d) UNITS cm^3(STP) cm^{-3} $atm^{-1/2}$

(For tritium, to convert to Ci $cm^{-3} T^{-1/2}$ multiply by 9.36×10^{-2})

(e) K_o and Q_k from Ref. 20 for inconel 625

S_o and Q_S from Ref. 21 for single crystal Ni

D_o and Q_D calculated from K_o, S_o, Q_k and Q_S

(f) Ref. 22

(g) Ref. 2, 23, 24

TABLE III

SUMMARY OF TRITIUM PERMEATION AND WALL LOADING
(All Quantities in Curies)

Discharge Cleaning - 72 Hours - Tritium Pressure = 10^{-3}T

Vacuum Vessel Element	Permeation			Wall Loading		
	20°C	150°C	250°C	20°C	150°C	250°C
Bellows	NEG	3	195	NEG	22	43
Plate Sections	NEG	NEG	NEG	63	16	71
Protective Plates	NA	NA	NA	NEG	NEG	NEG

NORMAL PULSED OPERATION - 1000 DISCHARGES $\tau = 300$ SEC
($\tau = 3 \times 10^4$ sec shown in parenthesis)

Vacuum Vessel Element	Permeation			Wall Loading		
	20°C	150°C	250°C	20°C	150°C	250°C
Bellows	NEG	NEG	NEG	NEG	NEG	NEG
Plate Sections	NEG	NEG	NEG	595 (59.5)	25 (2.5)	5 (.5)
Protective Plates	NA	NA	NA	150 (150)*	150 (150)*	150 (150)*

NEG = Negligible (< 1 Ci)

NA = Not applicable

*Values are upper limits. See discussion in Section V.

FIGURE CAPTIONS

Fig. 1. (783075) Graph of the noramlized total trapped tritium as a function of the dimensionless quantity αt where α is the rate coefficient.

Fig. 2. (783504) Graph of the normalized total quantity of tritium released from the outside wall of the vacuum vessel as a function of the dimensionless quantity αt where α is the rate coefficient.

Fig. 3. (783418) Implant distribution for charge-exchange tritium calculated in Ref. 18.

Fig. 4. (783420) Triangular approximation to the implant distribution in Fig. 3 which will be used in present calculations.

Fig. 5. (783417) Time behavior of implanted tritium for high power pulse operation and discharge cleaning.

Fig. 6. (783416) Graph of T_m in Eq. 41 normalized by $\tau/\Delta\tau$ as a function of the dimensionless variable $m^2\alpha\tau$. Plots are shown for various $\Delta\tau/\tau$. τ is the time between pulses, and $\Delta\tau$ is the duration of the pulse. α is the rate constant and m is the index of summation.

Fig. 7. (783419) Graph of X_m in Eq. 42 normalized by $d/(S_p c)$ as a function of mc/d. The constants are defined in Fig. 4.

Fig. 8. (783353) Graph of the normalized total quantity of tritium contained in a vacuum vessel component as a function of αt, where α is the rate constant and t is the time after which the source of tritium has been terminated. It is assumed that the trapped tritium at $t = 0$ is in its steady state distribution.

Fig. 9. (783203) Graph of the total amount of tritium contained in the bellows during discharge cleaning with tritium pressure of 10^{-3}T at three wall temperatures.

Fig. 10. (783204) Graph of the total amount of tritium leaving the bellows outer surface during discharge cleaning with tritium pressure of 10^{-3}T at three wall temperatures.

Fig. 11. (783227) Graph of the total quantity of tritium contained in the plate sections during discharge cleaning with a tritium pressure of 10^{-3} T at three wall temperatures.

Fig. 12. (783225) Graph of the total quantity of tritium contained in the plate sections during discharge cleaning due to charge exchange implanted tritium at three wall temperatures.

Fig. 13. (783230) Graph of the total quantity of tritium contained in the plate sections due to charge exchange implanted tritium during a normal pulsed operation at two wall temperatures plus various outgassing modes. The time between shots is 300 second.

Fig. 14. (783228) Graph of the the total quantity of tritium contained in the plate sections due to charge exchange implanted tritium during normal pulsed operation at 20°C plus two outgassing modes. The time between shots is 3×10^4 sec.

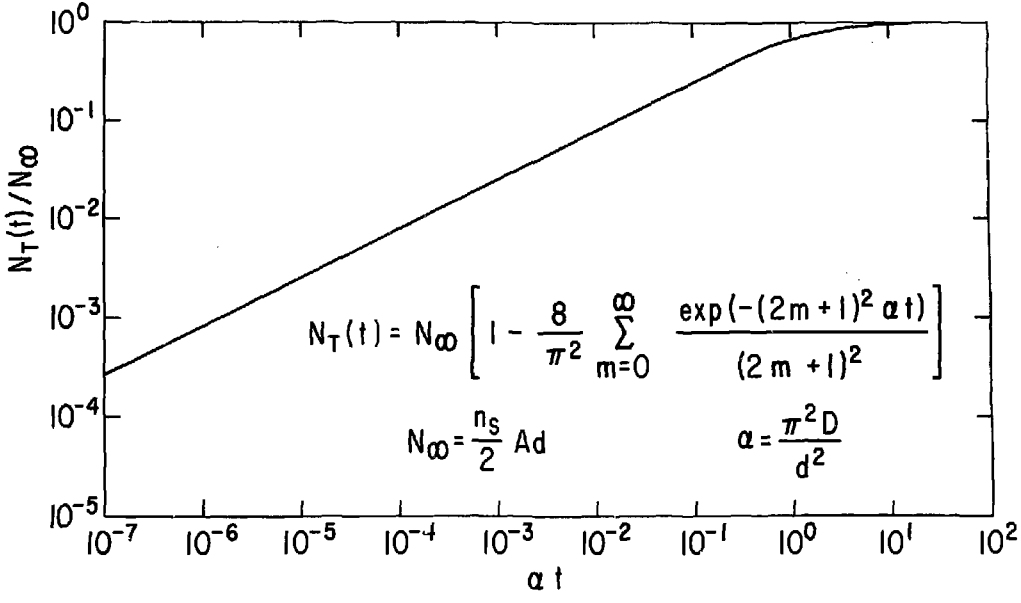
10^0
10^{-1}
10^{-2}
10^{-3}
10^{-4}
10^{-5}
$N_T(t)/N_\infty$
$N_T(t) = N_\infty \left[1 - \frac{8}{\pi^2} \sum_{m=0}^{\infty} \frac{\exp(-(2m+1)^2 \alpha t)}{(2m+1)^2} \right]$
$N_\infty = \frac{n_s}{2} Ad$
$\alpha = \frac{\pi^2 D}{d^2}$
10^{-7} 10^{-6} 10^{-5} 10^{-4} 10^{-3} 10^{-2} 10^{-1} 10^0 10^1 10^2
αt

Fig. 1. 783075

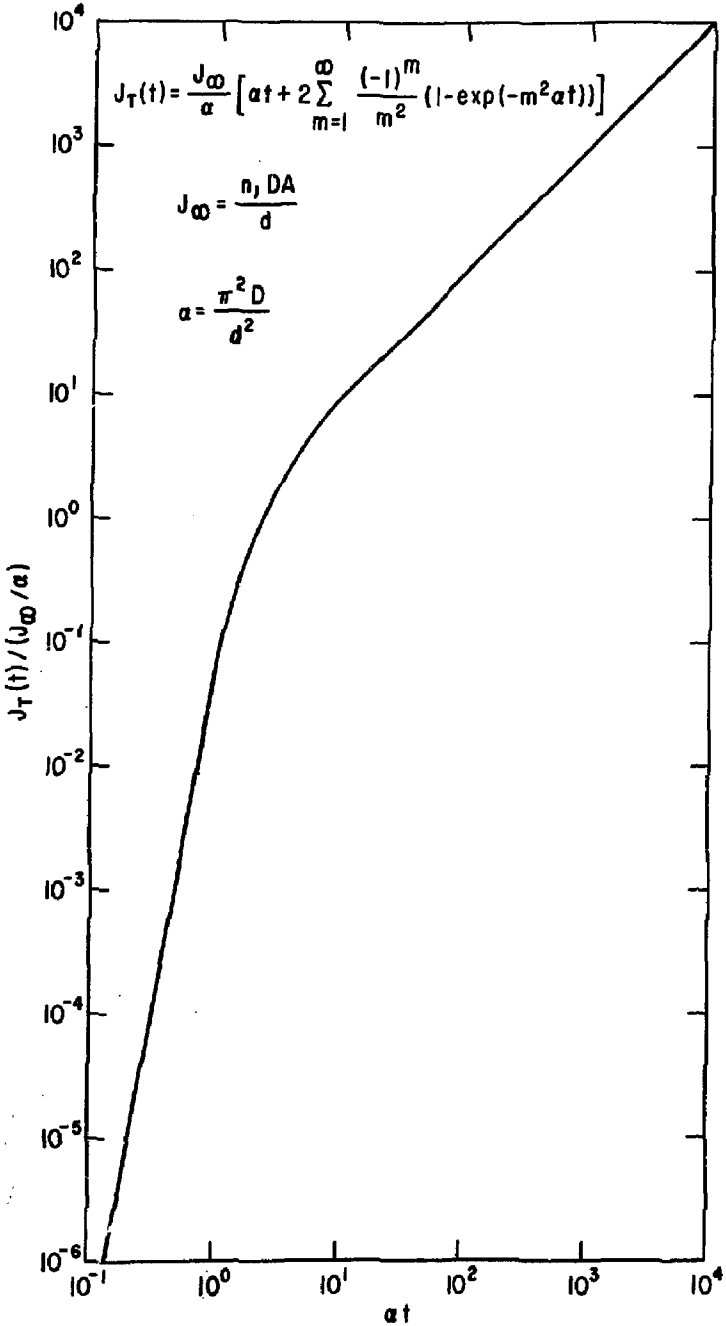
$J_T(t) = \frac{J_\infty}{\alpha}\left[\alpha t + 2\sum_{m=1}^{\infty}\frac{(-1)^m}{m^2}(1-\exp(-m^2\alpha t))\right]$
$J_\infty = \frac{n_1 DA}{d}$
$\alpha = \frac{\pi^2 D}{d^2}$
$J_T(t)/(J_\infty/\alpha)$
αt
10^{-6}
10^{-5}
10^{-4}
10^{-3}
10^{-2}
10^{-1}
10^{0}
10^{1}
10^{2}
10^{3}
10^{4}

Fig. 2. 783504

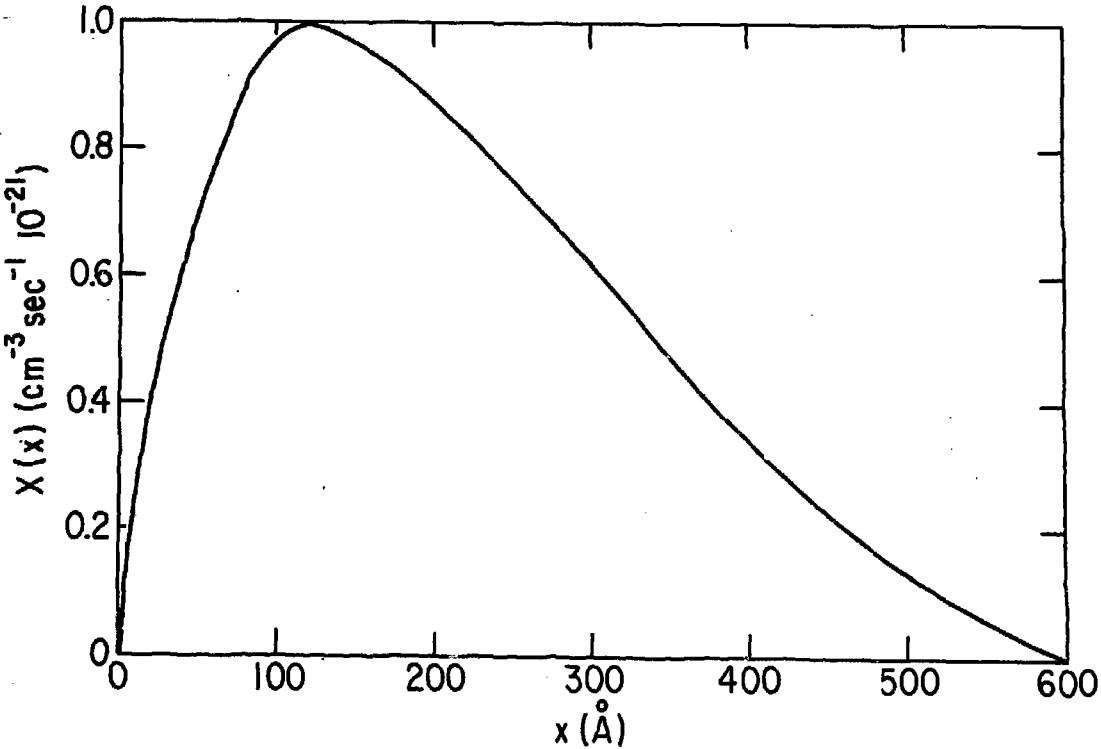

Fig. 3. 783418

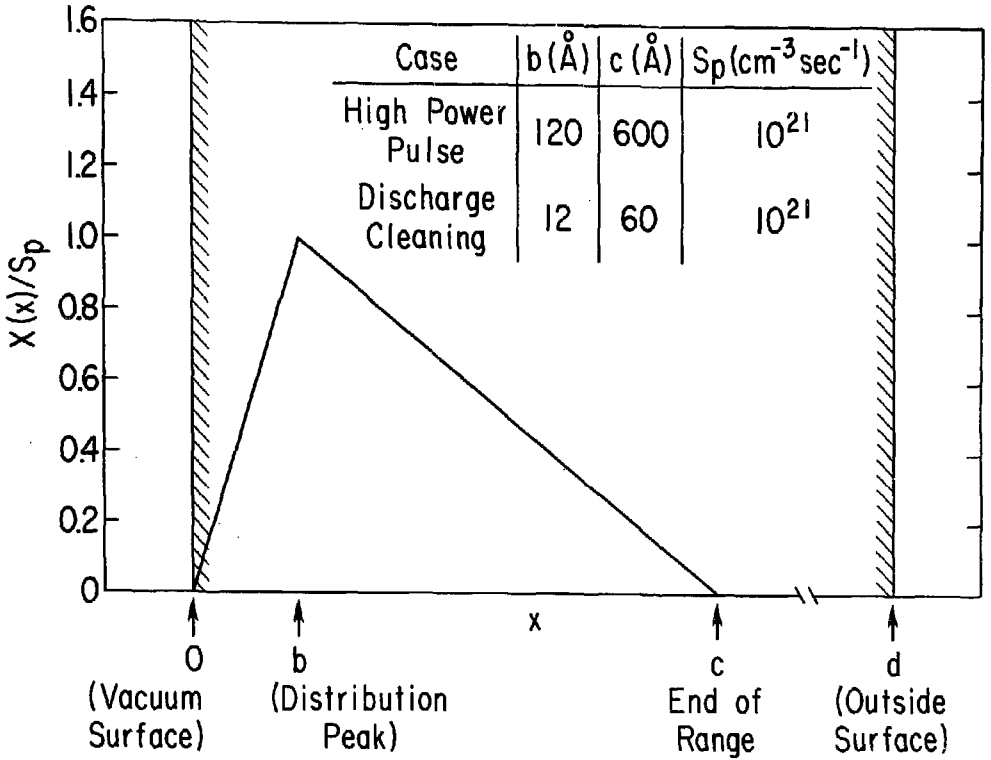
1.6
1.4
1.2
1.0
0.8
0.6
0.4
0.2
0
X(x)/Sp
Case
b(Å)
c(Å)
Sp(cm⁻³sec⁻¹)
High Power Pulse
120
600
10²¹
Discharge Cleaning
12
60
10²¹
x
0
(Vacuum Surface)
b
(Distribution Peak)
c
End of Range
d
(Outside Surface)

Fig. 4. 783420

Case	$\Delta\tau$ (sec)	τ (sec)
High Power Pulse	1	300
Discharge Cleaning	0.1	3

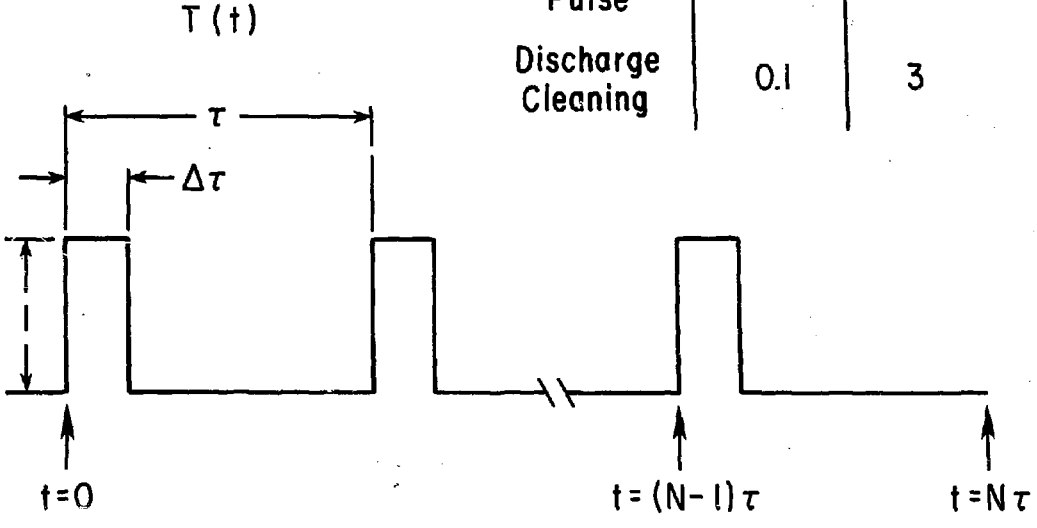

Fig. 5. 783417

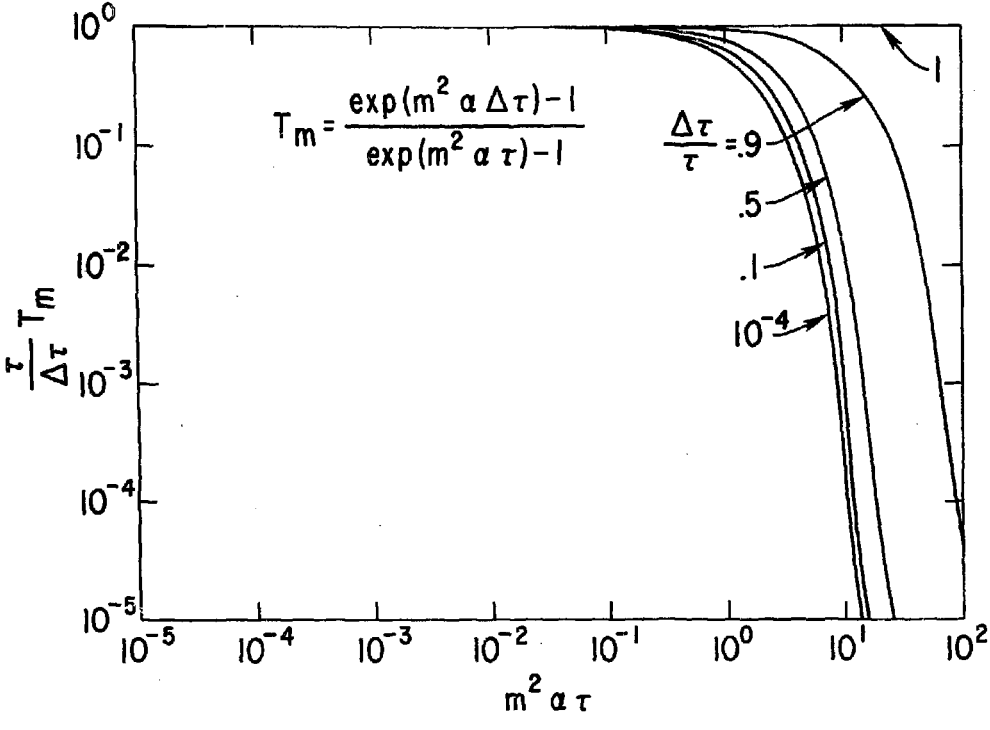
$T_m = \frac{\exp(m^2 \alpha \Delta\tau) - 1}{\exp(m^2 \alpha \tau) - 1}$
$\frac{\Delta\tau}{\tau}$ = .9
.5
.1
10^{-4}
1
$\frac{\tau}{\Delta\tau} T_m$
$m^2 \alpha \tau$
10^0
10^{-1}
10^{-2}
10^{-3}
10^{-4}
10^{-5}
10^{-5} 10^{-4} 10^{-3} 10^{-2} 10^{-1} 10^0 10^1 10^2

Fig. 6. 783416

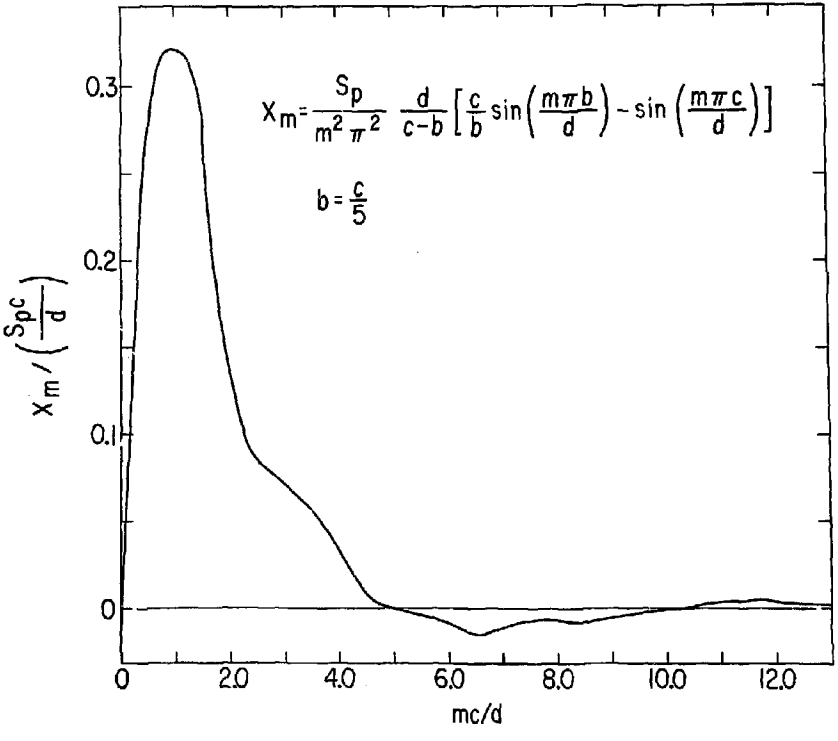
$X_m = \frac{S_p}{m^2\pi^2}\,\frac{d}{c-b}\left[\frac{c}{b}\sin\left(\frac{m\pi b}{d}\right) - \sin\left(\frac{m\pi c}{d}\right)\right]$
$b = \frac{c}{5}$
$X_m / \left(\frac{S_p c}{d}\right)$
0.3
0.2
0.1
0
0
2.0
4.0
6.0
8.0
10.0
12.0
mc/d

Fig. 7. 783419

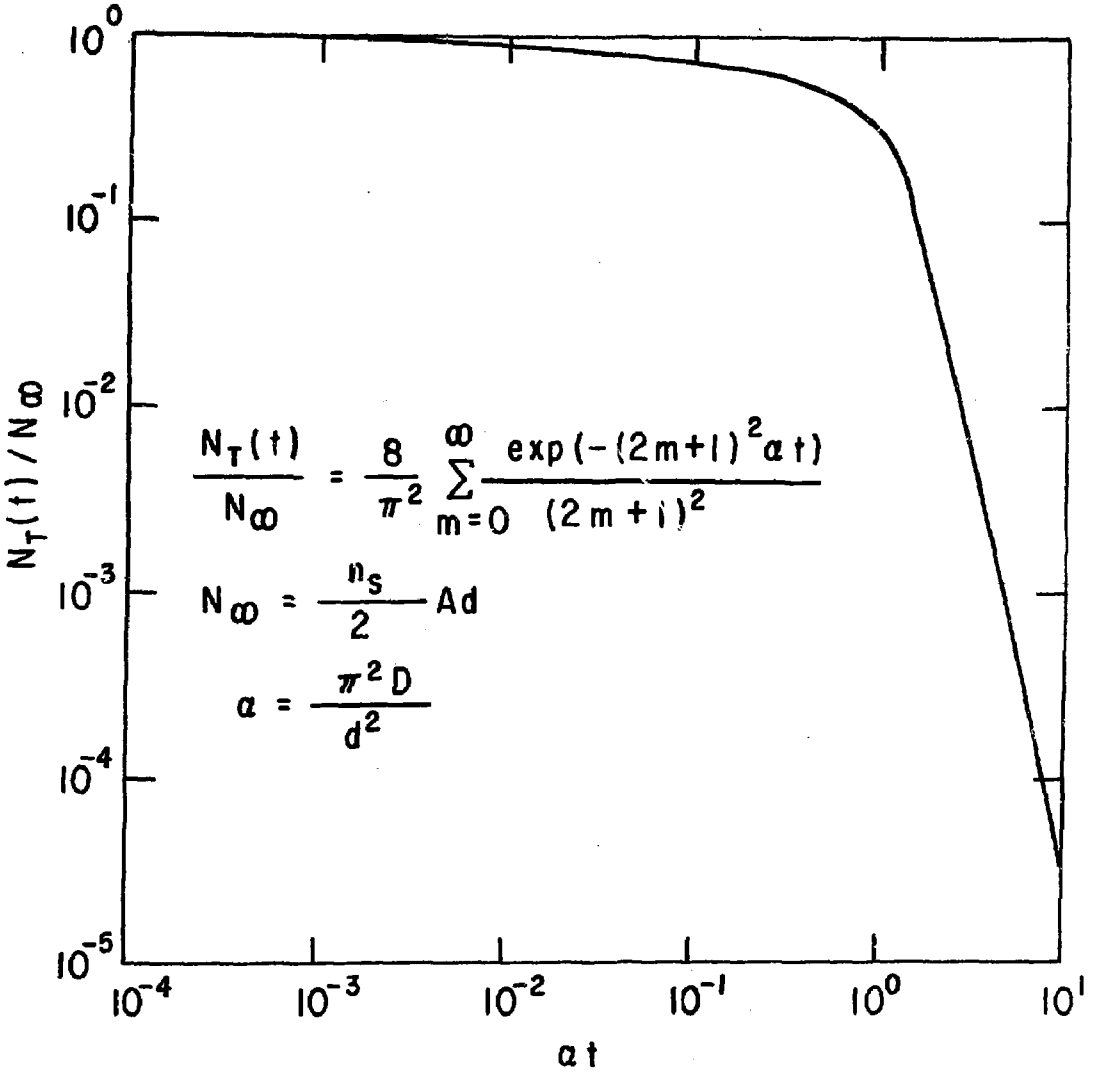
10^0
10^{-1}
10^{-2}
10^{-3}
10^{-4}
10^{-5}
$N_T(t) / N_\infty$
$\frac{N_T(t)}{N_\infty} = \frac{8}{\pi^2} \sum_{m=0}^{\infty} \frac{\exp(-(2m+1)^2 \alpha t)}{(2m+1)^2}$
$N_\infty = \frac{n_s}{2} Ad$
$\alpha = \frac{\pi^2 D}{d^2}$
10^{-4}
10^{-3}
10^{-2}
10^{-1}
10^0
10^1
αt

Fig. 8. 783353

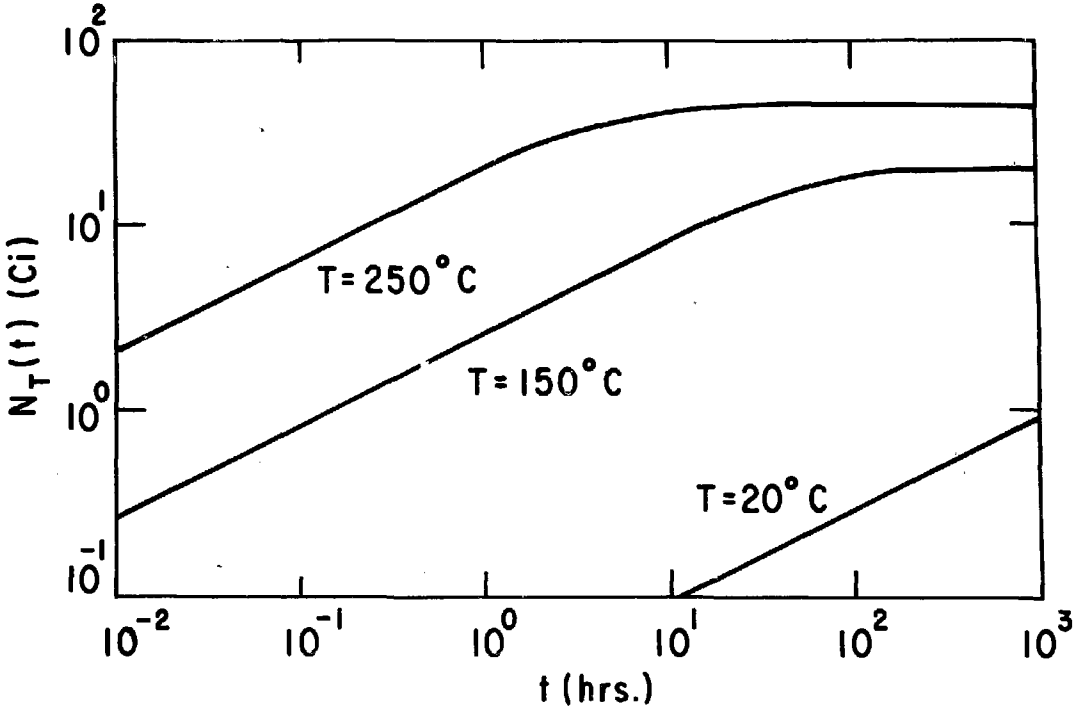
10^2
10^1
10^0
10^{-1}
$N_T(t)$ (Ci)
T=250°C
T=150°C
T=20°C
10^{-2}
10^{-1}
10^0
10^1
10^2
10^3
t (hrs.)

Fig. 9. 783203

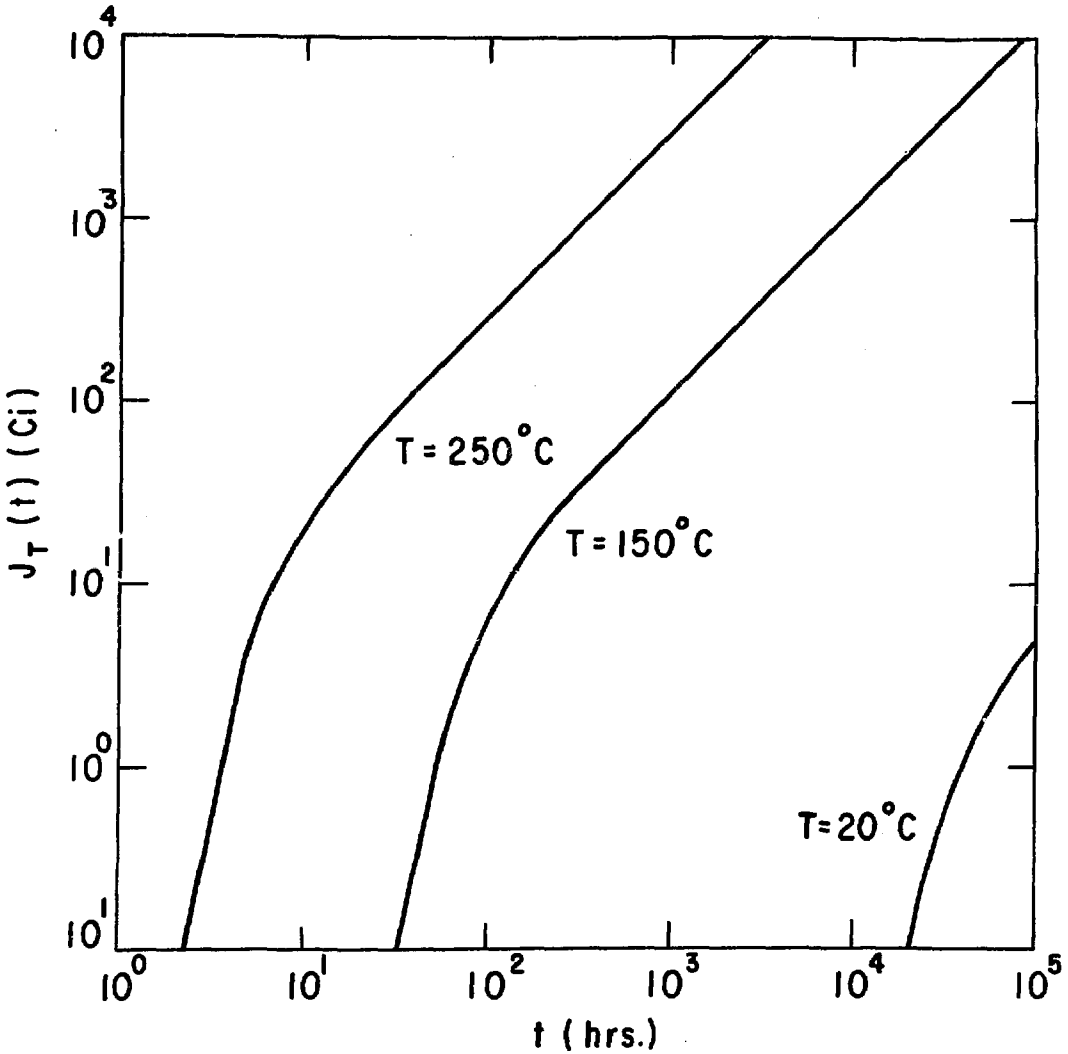

Fig. 10. 783204

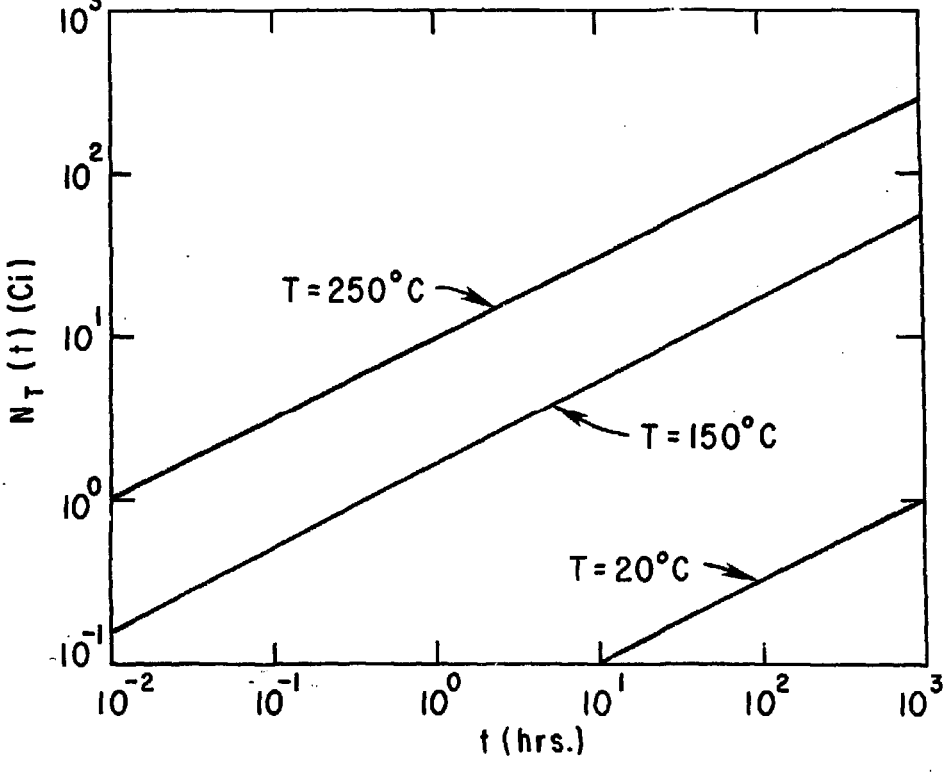

Fig. 11. 783227

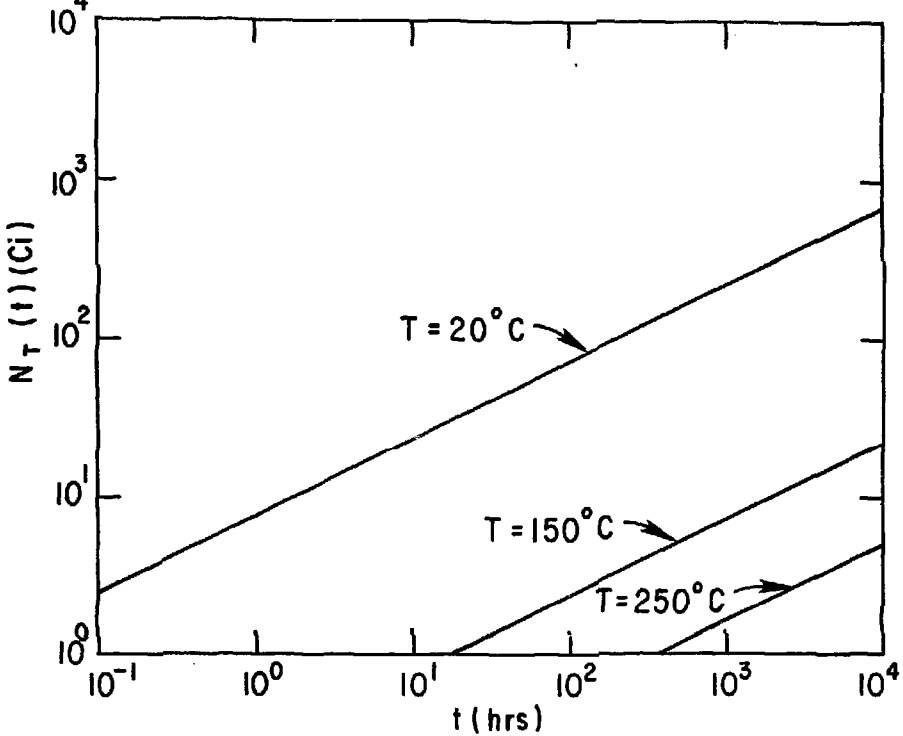

Fig. 12. 783225

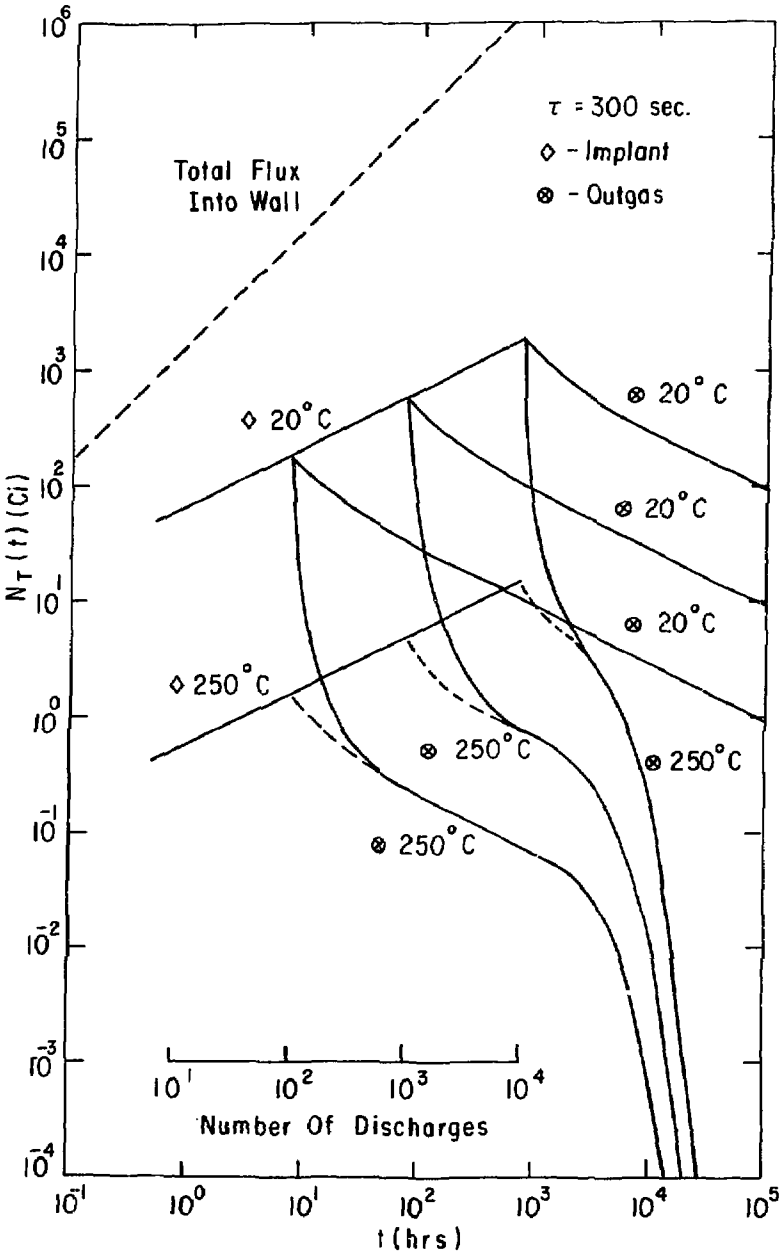

Fig. 13. 783230

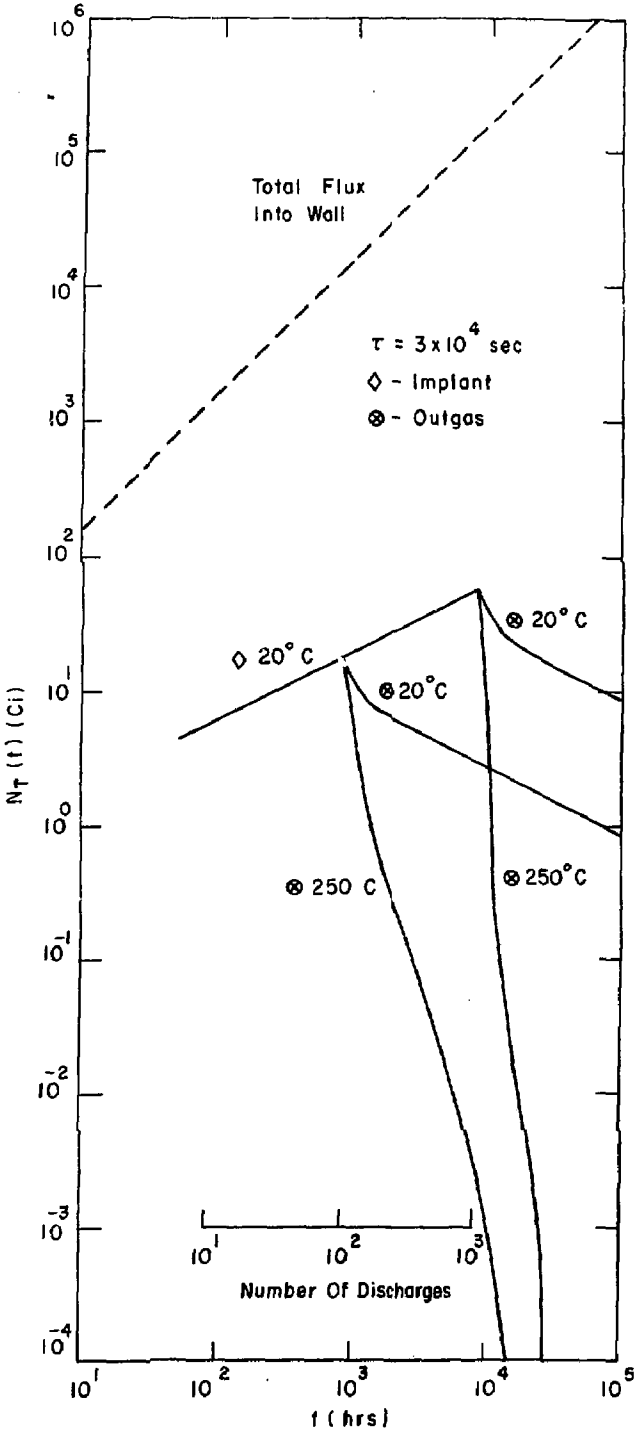

Fig. 14. 783228